ELSEVIER

Journal of Molecular Catalysis A: Chemical 114 (1996) 65–75

JOURNAL OF MOLECULAR CATALYSIS A: CHEMICAL

Preparation and photocatalytic studies on a novel Ti-substituted polyoxometalate

Nicholas J. Crano, R. Carlisle Chambers [1], Vincent M. Lynch, Marye Anne Fox *

The University of Texas at Austin, Department of Chemistry and Biochemistry, Austin, TX 78712, USA

Abstract

The crystal structure of a Ti-substituted Dawson-type polyoxotungstate $K_{19}H_9[P_4W_{32}Ti_6O_{132}]$ has been determined in the presence of coordinated oxalate anions. The K^+ salt is water soluble and the $[n\text{-}Bu_4N]^+$ salt is soluble in acetonitrile and acetone. The anion exists as a dimer of two $[P_2W_{16}Ti_2O_{62}]^{10-}$ units connected via two external TiO_6 octahedra. The photocatalytic activity of the $[n\text{-}Bu_4N]^+$ salt toward the oxidation of cyclohexanol, 1-hexanol, and 2-hexanol gave pseudo first-order rate constants of 0.03 h^{-1}, 0.01 h^{-1}, and 0.01 h^{-1}, respectively. The relative photocatalytic activities for the oxidation of cyclohexanol by $(n\text{-}Bu_4N)_9H_{19}[P_4W_{32}Ti_6O_{132}]$ and various polyoxotungstates of similar structure are compared.

Keywords: Polyoxotungstate; Titania; TiO_2; Homogeneous catalysis; Photooxidation

1. Introduction

Heterogeneously-dispersed metal oxide semiconductor particles have been used extensively as photocatalysts for the oxidation of organic compounds [1–3]. Photooxidation is of interest for environmental detoxification by oxidative degradation and for subsequent mineralization of organic contaminants [4,5]. Titanium dioxide (TiO_2), the most active semiconductor photocatalyst for this purpose, has been used broadly to degrade a wide variety of organic compounds [6–10]. The generally accepted mechanism for photooxidation by TiO_2 involves a pre-adsorption of the oxidizable substrate with the semiconductor surface, which is required for efficient interfacial electron transfer to effect electron or hole trapping. Unfortunately, this pre-association is difficult to study directly because of the heterogeneity of the adsorbate.

Early transition metal iso- and heteropolyoxoanions have many similarities with semiconductor metal oxide clusters and can be considered as soluble analogs of semiconductor metal oxide suspensions [11–13]. Oxoanions, such as $H_3PW_{12}O_{40}$ and $(n\text{-}Bu_4N)_4W_{10}O_{32}$, have also been used as photocatalysts for the photooxidation of organic compounds including alcohols [14,15], alkanes [16], and thioethers [17]. So far, the main limitation of polyoxometalates as photocatalysts is their lower quantum efficiency and catalytic activity when compared with particu-

* Corresponding author. Tel.: +1-512-4711811; fax: +1-512-4717791; e-mail: mafox@mail.utexas.edu.

[1] Current address: George Fox College, Department of Chemistry, Newberg, OR 97132

PII S1381-1169(96)00304-4

late TiO_2. An exception to this generalization is the isopolyoxoanion $[(n\text{-}Bu)_4N]_4W_{10}O_{32}$ [14,17]. On the basis of these observations, we speculated that incorporation of titanium atoms into the framework of a polyoxometalate might produce a highly efficient photocatalyst, and that the addition of a more active TiO_2-like site on the periphery of the polyoxometalate might increase the catalytic activity from that observed with the parent (unsubstituted) compound. We also hoped that the incorporated titanium oxide units might form a local aggregate resembling a TiO_2 q-particle [18,19], on which photooxidation might be even more efficient than on a TiO_2 colloid or particle. The structural inhomogeneity of the surface of this soluble anion might then lead to a greater understanding of the interactions taking place on the surface of a TiO_2 particle.

Finke et al. have previously reported the synthesis of a triply Ti-substituted silicotungstate $Si_2Ti_6W_{18}O_{77}^{14-}$ (**1**), based on the Keggin structure, as a dimer of two A-$SiTi_3W_9O_{40}^{10-}$ units connected by three Ti–O–Ti bonds (Fig. 1) [20]. This structure can be assembled conceptually by the removal of three corner-shared

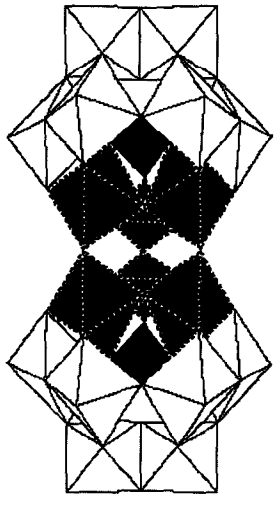

1

Fig. 1. The $Si_2W_{18}Ti_6O_{77}^{14-}$ (**1**), the Ti-substituted silicotungstate dimer [18].

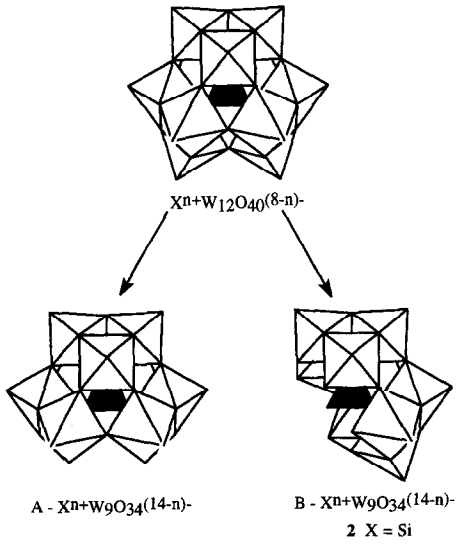

Fig. 2. Removal of three WO_6 octahedra from the parent Keggin anion $X^{n+}W_{12}O_{40}^{(8-n)-}$ to form the A- and B-type lacunary anions. When X = Si, the B-type anion is the lacunary anion **2**.

WO_6 octahedra from the $SiW_{12}O_{40}^{4-}$ Keggin anion [11] to form the A-type lacunary anion A-$SiW_9O_{34}^{10-}$ (Fig. 2). In contrast, the removal of three edge-shared octahedra would lead to formation of the B-type anion. Thus, Finke's compound is based on the A-type lacunary anion. Replacement of the lacunary sites by TiO_6 octahedra then gives the dimer $Si_2Ti_6W_{18}O_{77}^{14-}$.

Compound **1** showed very low photocatalytic reactivity in the presence of simple alcohols. Generally, substitution of one or more of the tungsten atoms by a lower valent transition metal, such as V or Nb, leads to lower photocatalytic activity [14]. The explanation for this is two-fold. First, previous photocatalytic studies of polyoxometalates have shown that, as with TiO_2, precomplexation of a substrate with the polyoxoanion is required for efficient photooxidation [14,21,22]. The addition of lower valent transition metals produces a higher net negative charge in the anion, which could lead to weaker pre-adsorption of substrate. Second, the greater dispersed negative charge on the catalyst may also inhibit further reduction of the anion [17]. Although the three TiO_6 octahedra of **1** resemble an extremely small TiO_2 particle,

nearly no photocatalytic activity is seen with **1**, possibly because the Ti active sites are effectively blocked from association with organic substrates because of the dimeric structure. Attempts to isolate the monomer of **1** have so far been unsuccessful.

In an effort to provide free access to potentially photoactive titanium sites, it would be desirable to substitute Ti octahedra into the B-type lacunary anion B-$SiW_9O_{34}^{10-}$ (**2**) (Fig. 2). Since the terminal Ti–O bonds in the A-type lacunary anion are almost parallel, head-to-head dimer formation is possible. In contrast, the terminal Ti–O bonds in a Ti-substituted B-type anion would be pointed away from each other, so as to avoid head-to-head dimerization, although dimerization through one Ti–O–Ti bridge could still occur.

Unfortunately, **2** is not yet known and attempts in our laboratory to insert Ti into the analogous compound B-$PW_9O_{34}^{9-}$ have been unsuccessful. However, it has proved possible to remove three edge-shared WO_6 octahedra from the Dawson-type (Fig. 3) polyoxotungstate $K_6P_2W_{18}O_{62} \cdot 14H_2O$ (**3**) to form the lacunary polyoxotungstate $Na_{12}P_2W_{15}O_{56} \cdot 19H_2O$ (**4**) [23]. Addition of **4** to an acidified solution of $K_2[TiO(C_2O_4)_2] \cdot H_2O$ or $TiOSO_4$ has led to the formation of the Ti-substituted anion $[P_4W_{32}Ti_6O_{132}]^{28-}$ (**5**) with an unusual structure: X-ray crystallographic analysis of the oxalate complexed anion $[P_4W_{32}Ti_6O_{124}(C_2O_4)_4]^{20-}$ shows a dimer made up of two $[P_2W_{16}Ti_2O_{62}]^{10-}$ units connected via two external TiO_6 octahedra, (Fig. 4). The absence of oxalate anions in the purified anion **5** is supported by elemental analysis. Herein, we report the synthesis and characterization of $K_{19}H_9[(P_4Ti_6W_{32}O_{132}) \cdot 33H_2O$ (**K5**) and $(n\text{-}Bu_4N)_9H_{19}[P_4W_{32}Ti_6O_{132}]$ (**Q5**). Initial photocatalysis studies are reported in which **Q5** is used to induce the oxidation of three simple alcohols.

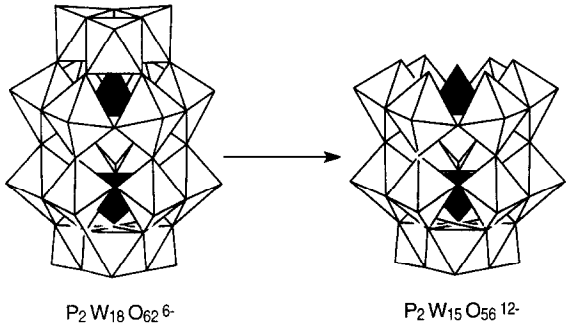

3 4

Fig. 3. Removal of three edge-sharing octahedra from the parent Dawson anion $P_2W_{18}O_{62}^{6-}$ (**3**) to form the lacunary anion $P_2W_{15}O_{56}^{12-}$ (**4**).

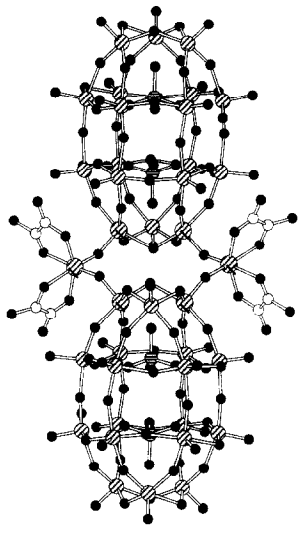

5

Fig. 4. View of the dimeric polyoxometalate anion $(P_4Ti_6W_{32}O_{132})^{28-}$ (**5**) in the presence of coordinating oxalate ligands.

2. Experimental

2.1. Materials

The polyoxotungstates $K_6P_2W_{18}O_{62} \cdot 14H_2O$, $Na_{12}P_2W_{15}O_{56} \cdot 19H_2O$, $H_3PW_{12}O_{40}$, $(n\text{-}Bu_4N)_4W_{10}O_{32}$, and $(n\text{-}Bu_4N)_9P_2W_{15}Nb_3O_{62}$ were prepared and purified by literature procedures [23,24]. This route produces a sample of $(n\text{-}Bu_4N)_9P_2W_{15}Nb_3O_{62}$ that is 95% pure by ^{31}P NMR. $K_2[TiO(C_2O_4)_2] \cdot H_2O$ (Aesar), and

(n-Bu_4N)PF_6 (Southwestern Analytical) were recrystallized from boiling H_2O. KBr, (n-Bu_4N)Br, and $TiOSO_4$ were used as received. Acetonitrile, cyclohexanol, 1-hexanol, and 2-hexanol used in the kinetics studies were distilled before use. Chlorobenzene and cyclohexanone were used as received.

Infrared (IR) spectra were obtained on a Nicolet 205 FT-IR spectrometer using 2–4% w/w KBr pellets. A Nicolet 360 MHz spectrometer was used to record ^{31}P NMR spectra using a broadband probe tuned to 71.1 MHz and the samples were referenced to 85% H_3PO_4 in D_2O. Ultraviolet (UV) spectra were obtained on a Hewlett Packard 8451A diode array absorption spectrophotometer. Cyclic voltammetry and bulk electrolysis were performed on a BAS-100 electrochemical analyzer. For cyclic voltammetry, Pt working and counterelectrodes referenced to $Ag^+/AgCl$ and [(n-$Bu)_4N$]PF_6 as supporting electrolyte (0.1 M) were used. Bulk electrolysis was performed under nitrogen with the same apparatus, but using a spongy carbon source as the working electrode. Thermal gravimetric analysis (TGA) was performed using a Perkin-Elmer TGA7 Thermogravimetric Analyzer. Elemental analyses were obtained from Galbraith Laboratories, Knoxville, TN.

Polyoxometalate and control solutions were irradiated in a Rayonet Photochemical reactor equipped with a cyclic array of low-pressure mercury arcs blazed at 300 nm. Product analysis of the irradiated solutions was conducted on a Hewlett Packard (HP) 5890 gas chromatograph (GC) equipped with a 25 m × 0.2 cm Carbowax DB-5 capillary column. The organic products were identified and quantified with an HP 3393A integrator.

2.2. Photolysis reactions

In a typical photolysis reaction, the polyoxometalate photocatalyst was added to 2 mL of a CH_3CN solution made 0.005, 0.025, 0.05, or 0.075 M in cyclohexanol in a quartz cuvette. Chlorobenzene (2×10^{-4} M) was used as an internal standard. The headspace of the cuvette was displaced by O_2 at which point the reaction vessel was capped with a cuvette cap wrapped with Teflon tape and sealed with parafilm. Samples were illuminated from 1–4 h, at which point they were allowed to cool to RT and analyzed by GC.

2.3. Preparation of $K_{19}H_9[(P_4Ti_6W_{32}O_{132}) \cdot 33H_2O$ (K5)

Method A: Preparation from $K_2[TiO(C_2O_4)_2] \cdot H_2O$: $K_2[TiO(C_2O_4)_2] \cdot H_2O$ (1.25 g, 3.53 mmol) was dissolved in 100 mL H_2O at RT and the solution was adjusted to a pH < 1 with 6 M HCl. To this rapidly stirred solution was added 5.00 g $Na_{12}P_2W_{15}O_{56} \cdot 19H_2O$ [23] (1.15 mmol) slowly in small portions. After stirring for 1 h, the solution was filtered through a fine frit funnel and 10 g KBr (excess) were added. The crude product precipitated immediately. The resulting slurry was allowed to stir for 15 min and the solid was allowed to settle for 1 h. The product was then filtered and the white solid was recrystallized from pH = 2.0 boiling H_2O at least three times to afford 2.90 g (51.7%) of the white powder $K_{19}H_9[(P_4Ti_6W_{32}O_{132}) \cdot 33H_2O$ (**K5**).

Infrared: 1085 (s), 1010 (w), 943 (s), 913(m), 828 (s), 782 (s), 683 (s), 524 (m) cm^{-1}. ^{31}P NMR (D_2O, pD = 1.5, 7.17 MHz): −7.35, −13.29 ppm. Elemental analysis, calculated for $K_{19}H_9[(P_4Ti_6W_{32}O_{132}) \cdot 33H_2O$: K, 7.62; H, 0.77; P, 1.27; W, 60.33; Ti, 2.95; O, 27.06; found: K, 7.61; H, 0.67; P, 1.33; W, 60.46; Ti, 3.06; O, 26.87. TGA, calculated for $33H_2O$: 6.2%; found: 6.1%.

Method B: Preparation from $TiOSO_4$: It is also possible to produce $K_{19}H_9[(P_4Ti_6W_{32}O_{132}) \cdot 33H_2O$ using $TiOSO_4$ as the Ti precursor. To an acidified solution (pH ~ 0.7) of $TiOSO_4$ (1.00 g, 6.25 mmol, 5.5 eq.) in 100 mL H_2O was added 5.00 g $Na_{12}P_2W_{15}O_{56} \cdot 19H_2O$ (1.15 mmol) slowly, with rapid stirring. After 1 h, an excess of KBr (~ 10 g) was added and a white solid precipitated immediately. The product was

recrystallized from boiling pH = 2.0 H_2O and 2.00 g (35.8%) of pure **K5** were obtained, with identical IR and ^{31}P NMR as reported for **K5** from method A.

Elemental analysis, calculated for $K_{19}H_9[(P_4Ti_6W_{32}O_{132}) \cdot 33H_2O$: K, 7.62; H, 0.77; P, 1.27; W, 60.33; Ti, 2.95; O, 27.06; found K, 7.45; H, 0.64; P, 1.37; W, 60.16; Ti, 3.53; O, 26.85. TGA, calculated for $33H_2O$: 6.2%; found: 6.4%. It is noted that the elemental analyses reported above are not completely identical. However, our experience with analyses of these compounds indicate a significant error with identical samples giving different results for one or two elements. It is not known why this is the case.

2.4. Preparation of $[(n\text{-}Bu)_4N]_9H_{19}(P_4Ti_6W_{32}O_{132})$ (Q5)

Pure $K_{19}H_9[(P_4Ti_6W_{32}O_{132}) \cdot 33H_2O$ (1.69 g, 0.173 mmol) was dissolved in 20 mL acidified H_2O (pH ~ 2). (n-Bu_4N)Br (1.43 g, 4.44 mmol) was added to the stirred solution. A white solid precipitated immediately. The slurry was stirred for 30 min and the resulting product was filtered and washed with 100 mL (almost boiling) H_2O to remove any unreacted (n-Bu_4N)Br. The white solid obtained (1.53 g, 83.6%) was soluble in acetonitrile, giving a colorless solution.

Infrared: 1150 (w), 1090 (s), 1017 (w), 949 (s), 916 (m), 888 (m), 820 (s), 634 (s), 561 (m), 526 (m) cm^{-1}. ^{31}P NMR (CD_3CN, 7.17 MHz): −5.38, −10.12 ppm. In agreement with previous studies on (n-Bu_4N)$^+$ salts of polyoxometalates [23], TGA showed less than 0.1% weight loss due to H_2O. Elemental analysis, calculated for $[(n\text{-}Bu)_4N]_9H_{19}(P_4Ti_6W_{32}O_{132})$: C, 16.30; H, 3.23; N, 1.19; P, 1.17; W, 55.48; Ti, 2.71; O, 19.92; found C, 16.39; H, 3.04; N, 1.22; P, 0.99; W, 54.58; Ti, 2.86; O, 21.06.

2.5. X-ray structural analysis

Crystals of the oxalate complexed anion of **K5** ($[(P_2Ti_3W_{16}O_{62})_2(C_2O_4)_4]^{20-}$) grew as small colorless prisms by crystallization from pH = 2.0 H_2O to approximately 0.25 × 0.33 × 0.52 mm. The data were collected at −85°C on a Siemens P3 diffractometer, equipped with a Nicolet LT-2 low-temperature device and using a graphite monochromator with MoKα radiation (l = 0.71073 Å). Details of crystal data, data collection and structure refinement are listed in Table 1.

Three reflections (−2,0,−6; −2,4,3; 2,−4,−3) were remeasured every 97 reflections to monitor instrument and crystal stability. A smoothed curve of the intensities of these check reflections was used to scale the data. The scaling factor ranged from 0.960 to 1.03. The crystals apparently undergo some decomposition in the X-ray beam as the crystal was observed to gradually turn deep blue as the data collection progressed. The data were corrected for Lp effects and absorption. The absorption correction was based on carefully measured crystal dimensions. Data reduction, decay correction and absorption correction were performed using the SHELXTL/PC software package [25].

The structure was solved by direct methods and refined by full-matrix least-squares [25] on F [26] with anisotropic thermal parameters for the tungsten, titanium and potassium atoms. The oxygen, phosphorus and carbon atoms were refined isotropically. Attempts to refine these atoms anisotropically resulted in many non-positive definite atomic displacement parameters which were usually due to a negative U_{ii}.

Although the oxometalate cluster was well behaved during refinement, it was difficult to locate the potassium atoms amongst the solvate water molecules. The oxygen–potassium contacts, in the range of 2.7–3.1 Å, are very similar to the O · · · O contacts expected for associated water molecules. Identification was made on the basis of the refined U_{iso} for the atom. Peaks around the oxometalate cluster were initially assigned as oxygen atoms from water and are refined. When the isotropic atomic displacement parameter refined to a very low or negative

Table 1
Crystallographic data [a] for the anion $[(P_2Ti_3W_{16}O_{62})_2(C_2O_4)_4]^{20-}$

Formula	$C_4H_{100}K_4O_{95}Ti_3W_{16}$
fw	4922.08
a (Å)	12.680(2)
b (Å)	13.988(5)
c (Å)	23.886(6)
α (°)	92.99(3)
β (°)	95.78(2)
γ (°)	95.52(2)
V (Å^3)	4187(2)
Z	2
$F(000)$	4380
Crystal system	triclinic
Space group	$P\bar{1}$
T (°C)	−85
2θ range (°)	4–45
Scan speed (°/min) (1.4° ω scan)	6–12
ρ_{calc} (g/cc)	3.904
Reflections measured	11508
Unique reflections	10914
Decay correction	0.960–1.03
$R_{int}(F^2)$	0.144
μ (cm^{-1})	225.14
Crystal size (mm)	0.25×0.34×0.52
Transmission factor range	0.0227–0.0945
$R_w(F^2)$ [b]	0.223
$R(F)$ [c]	0.118
Goodness of fit, S [d]	1.920
Parameters	612
Max$\lvert\Delta/\sigma\rvert$	<0.1
Min, max peaks (e$^-$/Å^3)	−5.2, 6.1

[a] Data were collected on a Siemens P3 diffractometer, equipped with a Nicolet LT-2 low-temperature device and using graphite monochromatized MoKα radiation ($\lambda = 0.71073$ Å). Data were collected using ω scans with a scan range of 1.4° in ω. Lattice parameters were obtained from the least-squares refinement of 37 reflections with $9.0 < 2\theta < 18.9°$.

[b] $R_w = \{\sum w(|F_o|^2 - |F_c|^2)^2 / \sum w(|F_o|)^4\}^{1/2}$, where the weight, w, is defined as follows: $w = 1/\{\sigma^2(|F_o|^2) + (0.02 * P)^2 P\}$; $P = [1/3 * (\text{maximum of } (0 \text{ or } |F_o|^2) + 2/3 * |F_c|^2]$.

[c] The conventional R index based on F where the 6196 observed reflections have $F_o > 4(\sigma(F_o))$.

[d] $S = [\sum w(|F_o|^2 - |F_c|^2)^2/(n-p)]^{1/2}$, where n is the number of reflections and p is the number of refined parameters.

value, the atom type was then assigned as potassium. Oxygen atoms on the metal cluster were assumed to be covalently bound and non-hydrogenated; all peaks assigned as oxygen in the voids around the cluster were assumed to be associated water molecules.

The formula, $[W_{16}Ti_2O_{54}(PO_4)_2]_2Ti_2(C_2O_4)_4{-}K_8(H_2O)_{50}$, was assigned by minimizing the function, $\sum w(|F_o|^2 - |F_c|^2)^2$, where $w = 1/[(s(F_o))^2 + (0.02 * P)^2]$ and $P = (|F_o|^2 + 2|F_c|^2)/3$. Neutral atom scattering factors and values used to calculate the linear absorption coefficient are

Table 2
Bond lengths (Å) and angles (°) for the titanium atoms in the anion $[(P_2Ti_3W_{16}O_{62})_2(C_2O_4)_4]^{20-}$

1	2	3	1–2	1–2–3
O8P	Ti18	O18T	2.23(4)	172.(2)
O8P	Ti18	O31B		83.(2)
O8P	Ti18	O32B		88.(2)
O8P	Ti18	O34B		76.(2)
O18T	Ti18	O31B	1.75(4)	102.(2)
O18T	Ti18	O32B		98.(2)
O18T	Ti18	O34B		99.(2)
O18T	Ti18	O36B		95.(2)
O31B	Ti18	O32B	1.90(4)	86.(2)
O31B	Ti18	O34B		159.(2)
O31B	Ti18	O36B		88.(2)
O32B	Ti18	O34B	1.99(4)	93.(2)
O32B	Ti18	O36B		167.(2)
O34B	Ti18	O36B	1.91(4)	88.(2)
O36B	Ti18	O8P	1.89(5)	79.(2)
O8P	Ti17	O17T	2.33(5)	168.(2)
O8P	Ti17	O29B		87.2(15)
O8P	Ti17	O30B		82.(2)
O8P	Ti17	O35B		78.(2)
O17T	Ti17	O29B	1.73(4)	103.(2)
O17T	Ti17	O30B		103.(2)
O17T	Ti17	O35B		97.(2)
O17T	Ti17	O36B		97.(2)
O29B	Ti17	O30B	1.95(3)	84.(2)
O29B	Ti17	O35B		88.(2)
O29B	Ti17	O36B		159.(2)
O30B	Ti17	O35B	1.94(5)	159.(2)
O30B	Ti17	O36B		89.(2)
O35B	Ti17	O36B	2.01(5)	91.(2)
O36B	Ti17	O8P	2.13(5)	73.(2)
O18T	Ti1	O1C	1.85(4)	93.(2)
O18T	Ti1	O2C		171.(2)
O18T	Ti1	O5C		104.(2)
O18T	Ti1	O6C		95.(2)
O17T′	Ti1	O18T	1.86(4)	94.(2)
O17T′	Ti1	O1C		103.(2)
O17T′	Ti1	O2C		90.(2)
O17T′	Ti1	O5C		91.(2)
O17T′	Ti	O6C		95.(2)
O1C	Ti1	O2C	1.94(5)	79.(2)
O1C	Ti1	O5C		157.(2)
O6C	Ti1	O1C	2.12(5)	88.(2)
O2C	Ti1	O5C	2.14(5)	83.(2)
O2C	Ti1	O6C		82.(2)
O5C	Ti1	O6C	2.06(5)	77.(2)

Table 3
Metal–metal contacts (Å) for the anion $[(P_2Ti_3W_{16}O_{62})_2(C_2O_4)_4]^{20-}$

1	2	1–2	1	2	1–2
W1	W2	3.441(4)	W1	W3	3.394(4)
W2	W3	3.369(5)	W1	W5	3.701(4)
W1	W6	3.695(4)	W2	W7	3.689(4)
W2	W8	3.678(4)	W3	W4	3.698(4)
W3	W9	3.687(4)	W4	W5	3.347(4)
W4	W9	3.741(4)	W4	W10	3.731(4)
W5	W6	3.683(4)	W5	W11	3.734(4)
W6	W7	3.399(4)	W6	W12	3.734(4)
W7	W8	3.694(4)	W7	W13	3.735(4)
W8	W9	3.327(4)	W8	W14	3.726(4)
W9	W15	3.733(4)	W10	W11	3.373(4)
W10	W16	3.712(4)	W10	W15	3.690(4)
W11	Ti17	3.611(12)	W11	W12	3.608(4)
W12	Ti17	3.591(12)	W12	W13	3.416(4)
W13	Ti18	3.592(12)	W13	W14	3.647(4)
W14	Ti18	3.592(12)	W14	W15	3.345(4)
W16	Ti17	3.292(12)	W15	W16	3.734(4)
Ti17	Ti18	3.357(16)	W16	Ti18	3.255(12)
Ti1	Ti18	3.428(17)	Ti1	Ti17	3.455(16)

from the International Tables for X-ray Crystallography (1990) [27]. Other computer programs used in this work are listed elsewhere [28]. All figures were generated using SHELXTL/PC [25]. Selected bond lengths and angles are listed in Table 2, and metal–metal distances in Table 3. Other crystallographic data is available as supplementary material.

3. Results and discussion

3.1. Characterization of $(P_4Ti_6W_{32}O_{132})^{28-}$ as the K^+ salt (K5) and as the $(n\text{-}Bu_4N)^+$ salt (Q5)

The Dawson–Wells phosphotungstate $Na_{12}P_2W_{15}O_{56}\cdot 19H_2O$ (**4**), which has three cluster vacancies, was added to an aqueous solution of the titanyl precursors $K_2[TiO(C_2O_4)_2]\cdot H_2O$ or $TiOSO_4$ at a pH ca. 1, thus generating the Ti-substituted polyoxoanion $(P_4Ti_6W_{32}O_{132})^{28-}$ (**5**). This purified anion has been isolated both as its water-soluble K^+ (**K5**) salt and its organic-solvent-soluble $[n\text{-}Bu_4N]^+$ salt (**Q5**). If the Ti precursor is $TiO(C_2O_4)_2$, the compound is at first isolated with coordinating oxalate anions to form the anion $[(P_2Ti_3W_{16}O_{62})_2(C_2O_4)_4]^{20-}$. These oxalate ligands can then be removed by repeated crystallization.

The ^{31}P NMR spectra of **Q5** is shown in Fig. 5. The fact that there are two resonances is evidence that the compound is pure and stable and that the C_{2h} symmetry of the dimer is intact. The chemical shifts are comparable with those from $P_2Nb_3W_{15}O_{62}^{9-}$ as well as other related complexes [13,23,24,29–31]. The wider gap between the two resonances in **Q5** when compared to **K5** is thought to be due to the interaction of the solvent with the Ti octahedra. With no oxalates present and in organic solvent, the Ti atoms may be partially coordinated by the solvent. This interaction should lead to a greater shift for one ^{31}P resonance.

As in the related Nb complexes, the IR spectrum resembles the $P_2W_{18}O_{62}^{6-}$ parent structure, but not the $P_2W_{15}O_{56}^{12-}$ starting material (Fig. 6). The stretch at 1130 cm^{-1} in the $P_2W_{15}O_{56}^{12-}$ spectrum has been assigned as a P=O stretch [23]. This band arises from the exposed phosphate group of the lacunary anion and disappears upon the incorporation of the Ti octahedra. These comparisons suggest that the Dawson–Wells skeleton is intact. That the absorbance at 1150 cm^{-1} reported for **Q5** is not due to this P=O stretch and is in fact due to the organic cation $[n\text{-}Bu_4N]^+$ can be seen by comparison with the IR spectra of $[n\text{-}Bu_4N]Br$. The

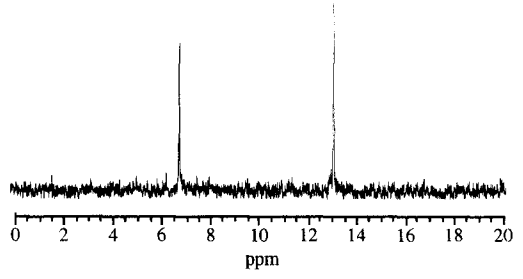

Fig. 5. The ^{31}P NMR spectrum of $[(n\text{-}Bu)_4N]_9H_{19}(P_4Ti_6W_{32}O_{132})$ (**Q5**) in CH_3CN referenced to H_3PO_4 in D_2O.

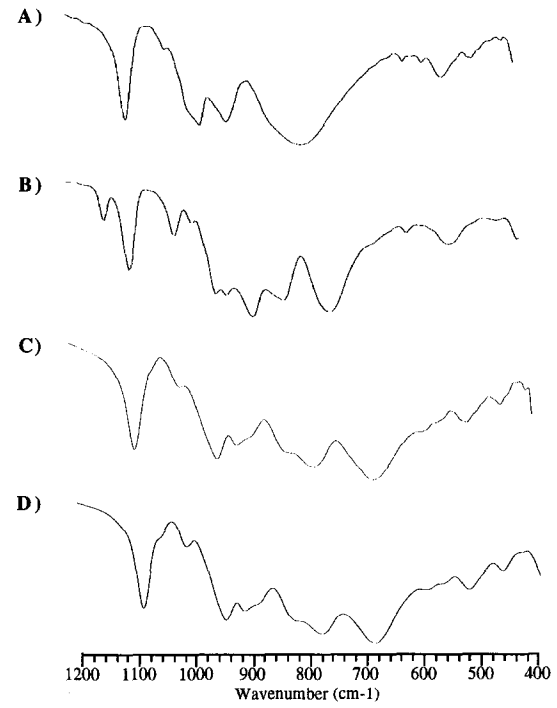

Fig. 6. IR spectra (KBr) of (A) $K_6P_2W_{18}O_{62}$, (B) $Na_{12}P_2W_{15}O_{56}\cdot 19H_2O$, (C) $K_{19}H_9[(P_4Ti_6W_{32}O_{132})\cdot 33H_2O$ from $K_2TiO(C_2O_4)_2$ (**K5**) and (D) **K5** from $TiOSO_4$.

band at 683 cm^{-1} in the product is assigned as the Ti–O–Ti bridging stretch by comparison with **1** [20]. This is also similar to the absorption at approximately 650 cm^{-1} that has been previously reported for an Nb–O–Nb bridge in

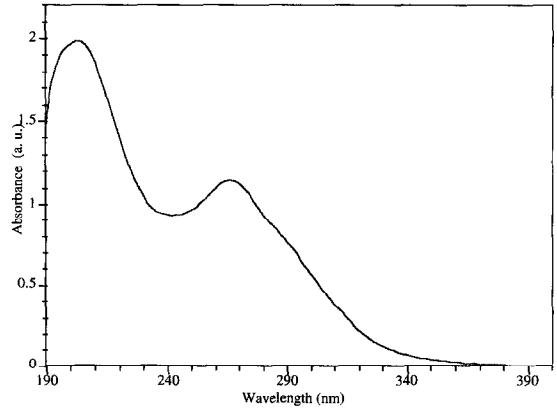

Fig. 7. UV absorption spectra of **K5** (4×10^{-6} M) in H_2O at pH = 4.

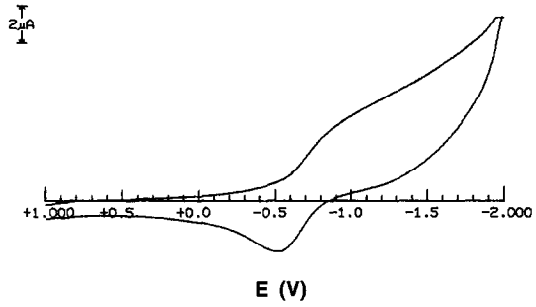

Fig. 8. Cyclic voltammogram of **Q5** in acetonitrile containing 0.1 M Bu_4NPF_6 as electrolyte on Pt. The scan rate was 200 mV/s. Bulk electrolysis showed this wave to be a 4 e^- reduction.

the related Nb-substituted Dawson-type phosphotungstate [23].

The UV absorption spectrum for both salts contains two bands at 200 ($\varepsilon = 600{,}000$) and 260 ($\varepsilon = 350{,}000$) nm as is shown for **K5** in Fig. 7. These bands are similar to those reported for other polyoxometalates as ligand-to-metal charge transfers (LMCT).

Cyclic voltammetry of the $(n\text{-}Bu_4N)^+$ salt (**Q5**) was performed in acetonitrile containing Bu_4NPF_6 as electrolyte (Fig. 8). A reversible wave is evident at approximately −800 mV. Bulk electrolysis under an inert atmosphere established that this wave signifies a 4 e^- reduction.

3.2. X-ray structure of $[P_4W_{32}Ti_6O_{124}(C_2O_4)_4]^{20-}$

The synthesis of the Dawson-type Ti-substituted dimer was based on the previous synthesis of A-β-$Si_2W_{18}Ti_6O_{77}^{14-}$ by Finke et al. [20]. Although the reaction of a Ti precursor with the lacunary Dawson-type polyoxotungstate $Na_{12}P_2W_{15}O_{56}\cdot 19H_2O$ was expected to give a triply Ti-substituted product similar to $Na_9P_2W_{15}Nb_3O_{62}$ [30], a different structure was obtained. Figs. 4 and 9 show the unusual structure corresponding to the oxalate complexed anion of **K5**, $[(P_2Ti_3W_{16}O_{62})_2(C_2O_4)_4]^{20-}$. This structure is unusual for two reasons. First, each monomer contains 16 W atoms, one more than the starting material, $(Na_{12}P_2W_{15}O_{56}\cdot 19H_2O)$.

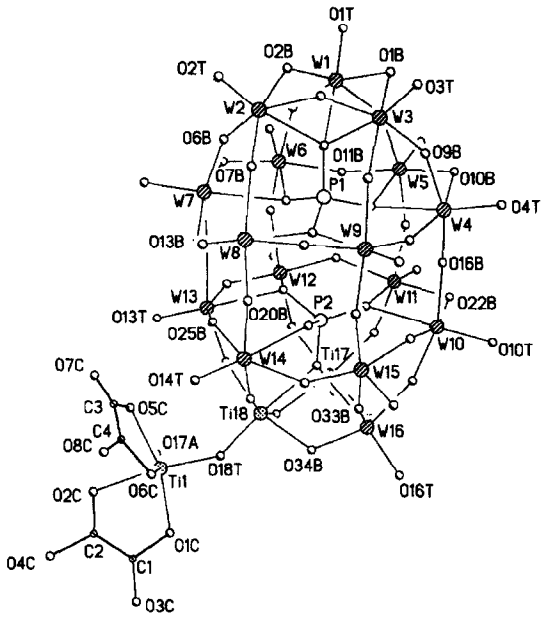

Fig. 9. View of the crystallographically unique half of the polyoxometalate complex $[(P_2Ti_3W_{16}O_{62})_2(C_2O_4)_4]^{20-}$, showing a partial atom labeling scheme. In the crystal, this complex exists as a dimer across a crystallographic inversion center at 1/2, 1/2, 0. The $W_{16}Ti_2O_{54}$ spheroidal shape moiety is bridged across this inversion center by two titanium bis-oxalates.

Second, only two Ti atoms are incorporated into each monomer, with two others connecting the monomer units. The extra W atom per each monomer probably derives from the decomposition of the starting material, for $Na_{12}P_2W_{15}O_{56} \cdot 19H_2O$ degrades to WO_4^{2-} and $P_2W_{18}O_{62}^{6-}$ fragments while standing in solution at room temperature in an NMR tube.

Titanium bond lengths for oxalate complexed **K5** are shown in Table 2 and metal–metal distances in Table 3. Other crystal data are contained in the supplementary material. As in most crystallographic studies of polyoxoanions [20,32], resolution was hindered by the high disorder of the cations and solvent of crystallization, although the core anion structure is firmly established. Repeated attempts at crystallization have been unsuccessful in producing higher quality crystals. Bond lengths around Ti are similar to those seen for previously reported anions **1** [20] and A-α-$Ge_2W_{18}Ti_6O_{77}^{14-}$ [33]. As expected, bond lengths and metal–metal distances for the $P_2W_{15}O_{56}$ units are similar to those reported for the salt $Na_{14}Cu[Cu_4(H_2O)_2(P_2W_{15}O_{56})_2 \cdot 53H_2O$ [32], with the average W–O bond distances: W–O (terminal) 1.69 Å (±0.07 Å); W–O (bridging) 1.90 (±0.12 Å); W–O (phos) 2.38 (±0.05 Å).

3.3. Loss of $(C_2O_4)^{2-}$ to form $(P_4Ti_6W_{32}O_{132})^{28-}$

Because **K5** was initially formed in the presence of oxalate anions, and because the X-ray structure showed these oxalates to be coordinated to the two outer Ti atoms, the formation of the Ti-substituted anion was attempted with a non-chelating counterion ($TiOSO_4$) as the Ti-precusor to determine whether a different oxide framework might be created in the absence of the coordinating ligand. The addition of **4** to a pH controlled aqueous solution of $TiOSO_4$, followed by the addition of KBr, produces a white powder that is spectroscopically equivalent to **K5** (Fig. 5d). Elemental analysis also indicates that the core structures of the products produced in the presence and absence of oxalate are identical. This constitutes proof that the main oxide framework of **K5** is unchanged by the preparation method. Elemental analyses of purified **K5** made both in the presence and absence of oxalate anion showed no detectable carbon, indicating the absence of oxalate anions in **K5** prepared via method A after multiple recrystallizations. Since the oxalate anion is not present in the purified material, we believe that the two bridging Ti atoms are coordinated by either OH or H_2O as in colloidal TiO_2.

3.4. Photocatalysis studies

The oxidation of cyclohexanol to cyclohexanone with **Q5**, $H_3PW_{12}O_{40}$ [15] and $(n\text{-}Bu_4N)_6P_2W_{18}O_{62}$ were similarly attempted. Table 4 shows the relative rate of photooxidative disappearance of cyclohexanol in acetonitrile induced by each of the above polyox-

ometalates. Under the reaction conditions employed, illumination with no catalyst present produced no photodegradation. Similarly, a reaction done in the presence of catalyst under reflux, but in the absence of light, showed no degradation. Lower activity is observed upon photocatalysis with **Q5** as the photocatalyst than with other polyoxometalate photocatalysts under identical reaction conditions and concentrations.

The apparent rate constants for the photocatalytic oxidations of a few simple alcohols by **Q5** are shown in Table 5, compared with those for the oxidation of cyclohexanol photocatalytically induced by $(n\text{-}Bu_4N)_6P_2W_{18}O_{62}$ and by $(n\text{-}Bu_4N)_9P_2W_{15}Nb_3O_{62}$. These apparent rate constants were calculated by the method of initial rates [34]. The oxidation of cyclohexanol by **Q5** was three times faster than the oxidation of either 1- or 2-hexanol under the same reaction conditions. Since the reaction probably entails H· abstraction, and thus radical formation [14,21], it is understandable that the rate constant is smaller for the primary alcohol 1-hexanol than for the secondary alcohol cyclohexanol. However, k_{obs} was smaller for 2-hexanol than cyclohexanol. Analogous effects observed with TiO_2 photocatalysis have been attributed to preferential adsorption of the less sterically encumbered alcohol on the photocatalytic surface [35].

Table 4
Relative photocatalytic oxidation of cyclohexanol in aerated acetonitrile by various polyoxometalate catalysts [a]

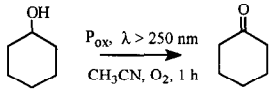

Polyoxometalate (P_{ox})	Relative % degradation
none	0.0
$H_3PW_{12}O_{40}$	1.0
$[(n\text{-}Bu)_4N]_4W_{10}O_{32}$	6.2
Q5	0.6

[a] Molar ratio of alcohol to photocatalyst was 10.

Table 5
Initial rate constants for the photocatalytic oxidation of alcohols by several polyoxometalates in aerated acetonitrile

Alcohol	Catalyst	Major product	k_{obs} ($h^{-1} \times 10^3$)
1-hexanol	**Q5**	hexanal	10
2-hexanol	**Q5**	2-hexanone	10
cyclohexanol	**Q5**	cyclohexanone	30
cyclohexanol	$(n\text{-}Bu_4N)_9P_2W_{15}Nb_3O_{62}$	cyclohexanone	2
cyclohexanol	$(n\text{-}Bu_4N)_6P_2W_{18}O_{62}$	cyclohexanone	4

The initial apparent rate constant for the photocatalytic oxidation of cyclohexanol by $(n\text{-}Bu_4N)_6P_2W_{18}O_{62}$ compared to that using $(n\text{-}Bu_4N)_9P_2W_{15}Nb_3O_{62}$ show a larger k_{obs} for the unsubstituted parent compound than is found for the Nb-substituted compound. This effect can be rationalized by the extra negative charge delocalization brought about by the Nb atoms, which in turn weakens pre-association of the alcohol with the catalyst. However, the contrasting increase in k_{obs} for the Ti-substituted polyoxometalate **Q5** over the unsubstituted and Nb-substituted compounds is evidence that substitution by Ti atoms does, in fact, increase the photocatalytic activity of the polyoxoanion, but not by the dramatic amounts that might be expected for a photoactive quantized particle.

4. Conclusions

Two new polyoxotungstates $[(n\text{-}Bu)_4N]_9H_{19}(P_4Ti_6W_{32}O_{132})$ (**Q5**) and $K_{19}H_9[(P_4Ti_6W_{32}O_{132})\cdot 33H_2O$ (**K5**) have been synthesized. The crystal structure of **K5** has been determined in the presence of coordinating oxalate ligands. $[(n\text{-}Bu)_4N]_9H_{19}(P_4Ti_6W_{32}O_{132})$ (**Q5**) is an active photocatalyst for the oxidation of simple alcohols, with the apparent rate constant for the oxidation of cyclohexanol as the Bu_4N^+ salt in acetonitrile showing a modest increase over that for the titanium-free parent compound $(n\text{-}Bu_4N)_6P_2W_{18}O_{62}$.

5. Supplementary material available

Crystallographic data including fractional atomic coordinates, anisotropic and isotropic thermal parameters, bond lengths and angles for the complete anion, and observed and calculated structure factor amplitudes are available from the author.

Acknowledgements

This work was supported by the U.S. Department of Energy, Office of Basic Energy Sciences and by the Robert A. Welch Foundation.

References

[1] M.A. Fox, Top. Current Chem. 159 (1991) 68.
[2] D.F. Ollis, E. Pelizzetti and N. Serpone, in: Photocatalysis: Fundamentals and Applications; N. Serpone and E. Pelizzetti (Eds.) (John Wiley and Sons, Inc., New York, 1989) pp. 603.
[3] M.A. Fox and M.T. Dulay, Chem. Rev. 93 (1993) 341.
[4] M. Schiavello, in: Photocatalysis and Environment. Trends and Applications, M. Schiavello (Ed.) (Kluwer Academic, Dordrecht, 1988) pp. 351.
[5] E. Pelizzetti, C. Minero, E. Borgarello, L. Tinucci and N. Serpone, Langmuir 9 (1993) 2995.
[6] W.G. Klemperer, in: Inorganic Synthesis, A.P. Ginsberg (Ed.), Vol. 27 (John Wiley and Sons, Inc., New York, 1990) ch. 3, pp 71.
[7] D. Duonghong, E. Borgarello and M. Grätzel, J. Am. Chem. Soc. 103 (1981) 4685.
[8] A. Henglein, Ber. Bunsenges. Phys. Chem. 86 (1982) 241.
[9] S. Yamagata, R. Baba and A. Fujishima, Bull. Chem. Soc. Jpn. 62 (1989) 1004.
[10] M. Gratzel, in: Photocatalysis: Fundamentals and Applications, N. Serpone and E. Pelizzetti (Eds.) (John Wiley and Sons, Inc., New York, 1989) pp. 123.
[11] M.T. Pope, Heteropoly and Isopoly Oxometalates (Springer-Verlag, Heidelberg, 1983).
[12] V.W. Day and W.G. Klemperer, Science 228 (1985) 533.
[13] R.G. Finke, M.W. Droege and P.J. Domaille, Inorg. Chem. 26 (1987) 3886.
[14] M.A. Fox, R. Cardona and E. Gaillard, J. Am. Chem. Soc. 109 (1987) 6347.
[15] K. Nomiya, T. Miyazaki, K. Maeda and M. Miwa, Inorg. Chim. Acta 127 (1987) 65.
[16] R.F. Renneke and C.L. Hill, J. Am. Chem. Soc. 110 (1988) 5461.
[17] R.C. Chambers and C.L. Hill, Inorg. Chem. 30 (1991) 2776.
[18] A. Henglein, Top. Current Chem. 143 (1988) 113.
[19] A. Henglein, Chem. Rev. 89 (1989) 1861.
[20] Y. Lin, T.J.R. Weakley, B. Rapko and R.G. Finke, Inorg. Chem. 32 (1993) 5095.
[21] C.L. Hill, D.A. Bouchard, M. Kadkhodayan, M.M. Williamson, J.A. Schmidt and E.F. Hilinski, J. Am. Chem. Soc. 110 (1988) 5471.
[22] C.L. Hill, R.F. Renneke and M.M. Williamson, Chem. Commun. (1986) 1747.
[23] D.J. Edlund, R.J. Saxton, D.K. Lyon and R.G. Finke, Organometallics 7 (1988) 1692.
[24] B.M. Rapko, M. Pohl and R.G. Finke, Inorg. Chem. 33 (1994) 3625.
[25] G.M. Sheldrick, SHELXTL/PC (Version 5.03) (Siemens Analytical X-ray Instruments, Inc., Madison, WI, 1994).
[26] H.D. Flack, Acta. Cryst. A 39 (1983) 876.
[27] A.J.C. Wilson (Ed.), International Tables for X-ray Crystallography, Vol. C, Tables 4.2.6.8 and 6.1.1.4 (Kluwer Academic Press, Boston, 1992).
[28] S.M. Gadol and R.E. Davis, Organometallics 1 (1982) 1607.
[29] R.G. Finke, B. Rapko, R.J. Saxton and P.J. Domaille, J. Am. Chem. Soc. 108 (1986) 2947.
[30] K. Nomiya, M. Kaneko, N.C. Kasuga, R.G. Finke and M. Pohl, Inorg. Chem. 33 (1994) 1469.
[31] R.G. Finke and M.W. Droege, J. Am. Chem. Soc. 106 (1984) 7274.
[32] T.J.R. Weakley and R.G. Finke, Inorg. Chem. 29 (1990) 1235.
[33] T. Yamase, T. Ozeki, H. Sakamoto, S. Nishiya and A. Yamamoto, Bull. Chem. Soc. Jpn. 66 (1993) 103.
[34] J.H. Espenson, Chemical Kinetics and Reaction Mechanisms, 2nd Ed. (McGraw-Hill, Inc., New York, 1995).
[35] M.A. Fox, H. Ogawa and P. Pichat, J. Org. Chem. 54 (1989) 3847.